High Performance Black Phosphorus Electronic and Photonic Devices with HfLaO Dielectric

Xiong Xiong, Xuefei Li, Mingqiang Huang, Tiaoyang Li, Tingting Gao, and Yanqing Wu

***Abstract*— As an emerging two-dimensional material, few-layer black phosphorus (BP) shows great potential in nanoelectronics and nanophotonics due to its high carrier velocity. However, non-optimized gate dielectrics often degrade the performance of BP devices severely. In this letter, we demonstrate high-performance BP devices using a novel HfLaO as back gate dielectric with improved interface quality. High current exceeding 1.15 mA/μm has been achieved at 20 K for BP transistors with improved noise spectral density. Moreover, BP photodetectors with a record high photoresponsivity up to 1.5 × 10^8 A/W and fast response time of 10 μs at 300 K are demonstrated. Excellent photoresponse in a broadband spectrum range from 514 to 1800 nm at 70 K has also been achieved.**

***Index Terms*— Black phosphorus, high-k, photoresponsivity, high field transport, low frequency noise.**

I. Introduction

OVER the past few years, emerging two-dimensional (2D) materials have attracted tremendous research efforts due to their extraordinary electronic and optical properties [1]–[12]. Few-layer BP, a new 2D elemental semiconductor with excellent carrier transport and optical properties have been extensively studied [13]–[15]. BP field-effect transistors (FETs) with high mobility up to ~1000 $cm^2V^{-1}s^{-1}$ has been demonstrated [16]. BP has a tunable direct bandgap from 2.0 eV (monolayer) to 0.3 eV (bulk), covering the optical spectrum range from visible to near infrared. These characteristics make BP a very promising candidate for broadband optoelectronic applications [17]–[19]. However, the current performance status of BP photodetectors in terms of broadband spectrum range, high photoresponsivity and fast response time is still unsatisfactory. Furthermore, the impurities and the dielectric environment have an important impact on the electrical and optical properties of BP devices. So far, most studies on BP devices use thick thermal SiO_2 film as a gate dielectric, and as a result, the low-quality interface typically degrades the device performance. Recently, there are some works have been reported focused on gate dielectric of BP devices [20]–[23]. In this work, we demonstrate high-performance BP transistors with high-quality atomic layer deposited HfLaO as back gate dielectric layer. Both electronic and optoelectronic performance of these devices are greatly improved compared with those using conventional thermal SiO_2 as gate dielectrics, owing to the improved interface quality with reduced surface charge scattering.

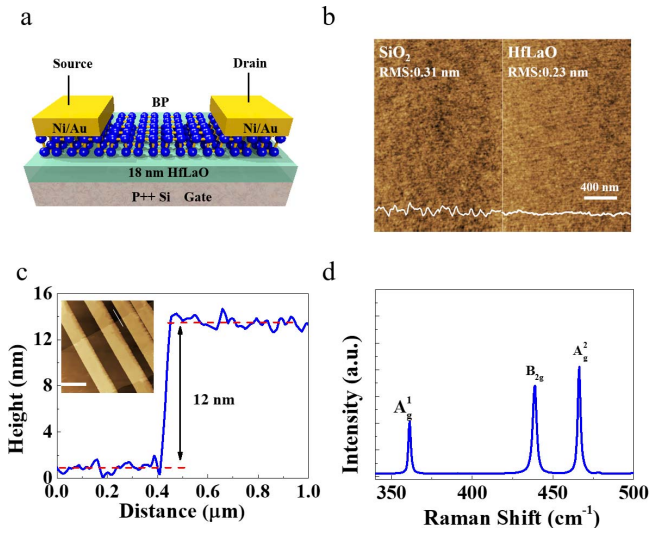

Fig. 1. (a) Schematic view of the device fabricated in this work. (b) AFM image of SiO_2 and HfLaO surfaces. (c) BP flake thickness measured by AFM is 12 nm. The scale bar is 1 μm. (d) Raman spectra of the BP film.

II. Device Fabrication

Layered BP flakes were mechanically exfoliated from bulk crystal and then transferred onto a Si substrate covered with a 90 nm thermal SiO_2 or 18 nm HfLaO dielectric layer grown by atomic layer deposition. The schematic view of the devices in this work is shown in Fig. 1a. The source/drain electrodes were patterned by electron beam lithography (EBL) and then 20 nm Ni/50 nm Au metal stack was deposited by e-beam evaporation. The capacitance density of the HfLaO layer is 0.85 μF/cm^2, corresponding to an equivalent oxide thickness (EOT) of 4 nm. The AFM top view image of the 90 nm

Manuscript received September 10, 2017; revised November 30, 2017; accepted November 30, 2017. Date of publication December 4, 2017; date of current version December 27, 2017. This work was supported by the National Natural Science Foundation of China (Grant Nos. 61574066, 61390504, and 11404118) and Hubei Provincial Natural Science Foundation of China (Grant Nos. 2016CFB414). The review of this letter was arranged by Editor K. M. Lau. *(Corresponding author: Yanqing Wu.)*

The authors are with the Wuhan National High Magnetic Field Center, School of Optical and Electronic Information, Huazhong University of Science and Technology, Wuhan 430074, China (e-mail: yqwu@mail.hust.edu.cn).

Color versions of one or more of the figures in this letter are available online at http://ieeexplore.ieee.org.

Digital Object Identifier 10.1109/LED.2017.2779877

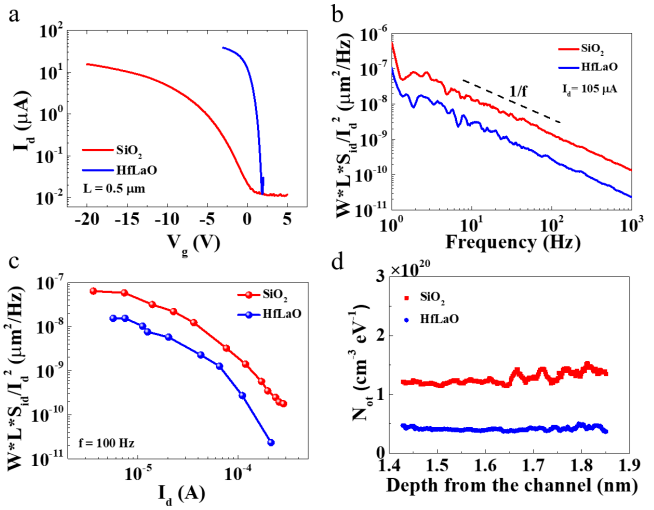

Fig. 2. (a) Transfer characteristics of the same channel length device with SiO_2 and HfLaO dielectrics at 300 K. V_d is −0.05 V. (b) Normalized noise spectral density as a function of frequency for SiO_2 and HfLaO at similar drain current. (c) Current spectral density S_{id}/I_d^2 at $f = 100$ Hz *versus* drain current I_d for the BP devices with SiO_2 and HfLaO at room temperature. (d) Oxide trap density distribution in dielectrics, extracted from the low-frequency noise spectra.

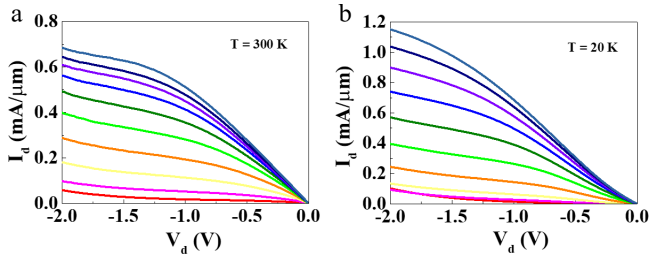

Fig. 3. The output characteristics of a 0.1 μm channel length BP device with HfLaO dielectric at 300 K (a) and 20 K (b).

SiO_2 and 18 nm HfLaO surfaces is shown in the left and right panel of Fig. 1b, respectively. The surface roughness root mean square (RMS) is 0.31 nm and 0.23 nm for SiO_2 and HfLaO, respectively. The BP flakes were identified by a combination of optical microscope and atomic force microscopy (AFM). A typical film thickness is around 12 nm as shown in Fig. 1c. Fig. 1d shows the Raman spectra of this flake where three characteristic Raman modes, A_g^1, B_{2g}, and A_g^2 can be observed, corresponding to the out-of-plane vibration (∼361 cm^{-1}), in-plane vibration along the zigzag (∼438 cm^{-1}) and armchair (∼466 cm^{-1}) directions [24], [25]. BP flakes with similar thickness were exfoliated on to substrates with HfLaO and SiO_2. Moreover, all devices based on HfLaO and SiO_2 were fabricated side by side with the same fabrication process and measured at the same time for a valid comparison.

III. Result and Discussion

The transfer characteristics of the devices with SiO_2 and HfLaO dielectrics with a channel length of 0.5 μm are shown in Fig. 2a. The subthreshold slope is ∼ 3.4 V/dec for the device based on $SiO_2$and ∼ 188 mV/dec for the device based on HfLaO. Low-frequency ($1/f$) noise is commonly used in conventional CMOS technology as an effective tool for evaluating the interface quality in field-effect transistors. We carried out a systematic investigation on $1/f$ noise of BP devices with HfLaO dielectric, and compare with the BP devices with the 90 nm SiO_2 dielectric. The $1/f$ noise was measured in the linear region at $V_d = -0.2$ V at 300 K for the 0.1 μm devices. The normalized noise spectral densities ($W \times L \times S_{id}/I_d^2$) of both devices as a function of frequency are shown in Fig. 2b at a similar drain current of 105 μA. The noise spectral densities follow the $1/f$ trend without generation-recombination bulge signatures. The noise level is lower for the device based on HfLaO. The normalized noise spectral densities of both devices are shown in Fig. 2c. $W \times L \times S_{id}/I_d^2$ has the same dependence on I_d for both devices, implying the same noise mechanism. The device on HfLaO dielectric shows a much lower noise level of $\sim 2.3 \times 10^{-11}$ μm^2 Hz^{-1} at 100 Hz about 10 times smaller than that of SiO_2. Moreover, the oxide trap density (N_{OT}) profile extracted by a distributed oxide trap model is shown in Fig. 2d [26], [27]. The N_{OT} of the HfLaO transistor is half of that using SiO_2. The interface state density (D_{it}) of $\sim 1.2 \times 10^{12}$ $eV^{-1}cm^{-2}$ and $\sim 4.7 \times 10^{11}$ $eV^{-1}cm^{-2}$ for SiO_2 and HfLaO device at 300 K was extracted by using the same approach as in [28]. These results suggest that HfLaO is an excellent dielectric for BP transistors with low N_{OT}, good quality interface and reduced low-frequency noise.

The high field transport of the short channel BP device with high-k dielectric has also been carried out. Fig. 3a and 3b show the output characteristics for the 100-nm channel length BP devices at 300 and 20 K, respectively. A maximum drain current (I_{dmax}) of 0.69 mA/μm is obtained at $V_d = -2$ V and $V_g = -3$ V, higher than previous values using chemical doping and vacuum annealing [29], [30]. At 20 K, the drain current increases up to 1.15 mA/μm at $V_d = -2$ V and $V_g = -3$ V.

The output characteristics of BP devices in the dark and under illumination are plotted in Fig. 4a. As expected, the current of transistors based on high-k dielectric is about 5 times larger than that on SiO_2 dielectric at similar carrier densities. To quantitatively analyze the photoresponse, we extract the photocurrent ($I_{ph} = I_{illumination}$-$I_{dark}$) data as shown in Fig. 4b. The photocurrent of BP device based on HfLaO is about 10 times larger than that on SiO_2 with the same device geometry. The photoresponsivity ($R = I_{ph}/P_{in}$) of the BP devices with different channel lengths have been investigated. As shown in Fig. 4c, R increases rapidly when the channel length scales from 1 μm to 0.1 μm. This is consistent with the photoconductive mechanism that transverse electric field increases in shorter channel devices. A high photoresponsivity of $\sim 1.2 \times 10^7$ A/W can be achieved for the BP device based on HfLaO, about 10 times higher than that based on SiO_2. Photoresponsivity under different incident laser power densities are also studied in Fig. 4d, where a record high photoresponsivity of 1.5×10^8 A/W is achieved at 300 K. [24], [25], [31]–[34]. The detectivity (D) of $\sim 4.5 \times 10^{14}$ $W^{-1}Hz^{1/2}$ and specific detectivity (D^*) of $\sim 2.1 \times 10^{10}$ Jones at a 633 nm wavelength can be extracted at HfLaO device of 100 nm channel length at room temperature using $D^* = (A\Delta f)^{1/2}R/i_n$ and $D = \Delta f^{1/2}R/i_n$, where A is

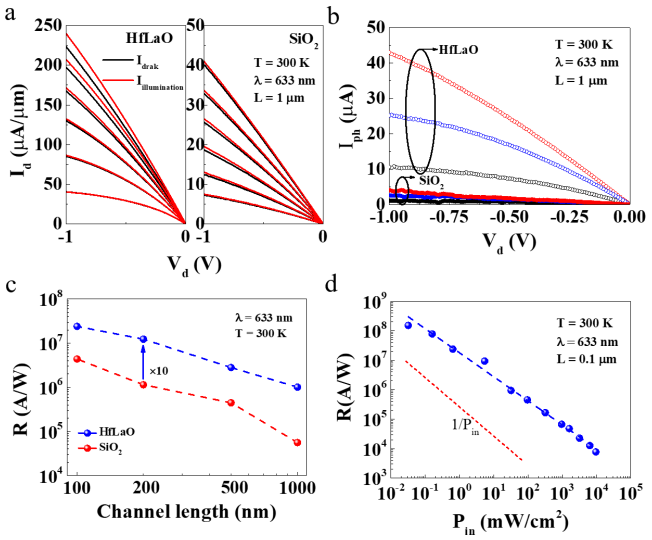

Fig. 4. (a) The output characteristics of the BP devices (channel length L = 1 μm) with 18 nm HfLaO dielectric (V_g from 0 V to −2.5 V) and 90 nm SiO_2 dielectric (V_g from 5 V to −20 V) at 300 K. The red and black line are the device under illumination (P_{in} = 250 mW/cm^2) and in the dark, respectively. (b) The comparison of device photocurrent with HfLaO dielectric and SiO_2 dielectric extract from (a). (c) R of devices with different channel lengths at room temperature. The laser is set to be the same (P_{in} = 0.6 mW/cm^2) for BP device with HfLaO dielectric and SiO_2 dielectric. (d) R versus different laser power at 300 K of BP device with HfLaO dielectric at V_g = −2.5 V and V_d = −2 V.

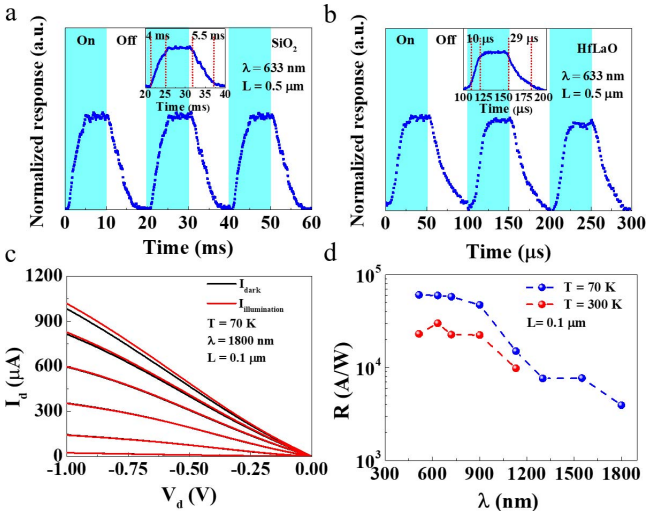

Fig. 5. Photoresponse time of a 0.5 μm channel length device based on (a) SiO_2 dielectric (b) HfLaO dielectric. The inset shows the rise and fall time for the photodetectors. (c) The output characteristics of the BP device with HfLaO dielectric at 70 K in the dark and under illumination of laser wavelength λ = 1800 nm and power P_{in} = 6000 mW/cm^2. (d) Photoresponsivity of the 0.1 μm device at different wavelengths at T = 300 K and T = 70 K while the incident power is fixed at 1600 mW/cm^2.

the effective area of the detector, R is the photoresponsivity, Δf is the bandwidth, i_n is noise current at the same bias condition with R[35].

The photoresponse time, a key figure of merit in photodetectors, has also been measured. The rise and fall time are defined as the time lapse between 10% to 90%. As shown in Fig. 5a, the extracted response time of BP device with SiO_2 dielectric at room temperature is τ_{rise} ∼4 ms, which is in the same order of magnitude from previous work using SiO_2 dielectric [18], [24], [34]. Also shown in Fig. 5b, BP device with HfLaO dielectric exhibits a much faster response time with τ_{rise} ∼10 μs, almost three orders of magnitude smaller than that of SiO_2. This fast response can be attributed to the shorter transit time of photogenerated carriers with improved interface capture and emission properties of photogenerated carriers. The response time of BP photodetectors is mainly limited by photocarrier recombination and carrier transport in the channel [33]. It can be further improved by higher mobility, better interface, smaller contact resistance, higher transverse electric field and possible design of thin vertical pn junctions. At longer wavelengths with T = 300 K, distinct photoresponse can no longer be observed beyond 1200 nm, which can be attributed to the drain current noise and jitter caused by shallow traps activated by thermal energy. When the temperature is decreased to 70 K, a large photocurrent of 36 μA can be obtained at a near-infrared wavelength of 1800 nm as shown in Fig. 5c. A wide photoresponse spectrum range from 514 nm to 1800 nm has been demonstrated at T = 70 K as shown in Fig. 5d. The photoresponsivity exhibits a decreasing trend from visible to near-infrared as expected from the smaller photon energy as laser wavelength increases.

IV. Conclusion

In conclusion, we have demonstrated high-performance BP based electronic and optoelectronic devices with a high-quality HfLaO film as the gate dielectric. Extraordinary performance enhancement in both electrical and optical properties can be achieved. High current of 1.15 mA/μm of a 100-nm device has been obtained at 20 K for the first time. High-performance photodetectors based on this novel dielectric has also been demonstrated with a record high photoresponsivity up to 1.5 × 10^8 A/W and a fast response time of 10 μs at 300 K. The reduced interface scattering leads greatly improved interface quality between HfLaO and black phosphorus channel. The promising results of this work show that performance improvement can be further explored using dielectric engineering for future electronics and optoelectronics.

References

[1] X. Li, L. Yang, M. Si, S. Li, M. Huang, P. Ye, and Y. Wu, "Performance potential and limit of MoS_2 transistors," *Adv. Mater.*, vol. 27, no. 9, pp. 1547–1552, Jan. 2015, doi: 10.1002/adma.201405068.

[2] K. F. Mak, K. He, C. Lee, G. H. Lee, J. Hone, T. F. Heinz, and J. Shan, "Tightly bound trions in monolayer MoS_2," *Nature Mater.*, vol. 12, no. 3, pp. 207–211, Dec. 2012, doi: 10.1038/nmat3505.

[3] K. F. Mak, K. He, S. Jie, and T. F. Heinz, "Control of valley polarization in monolayer MoS_2 by optical helicity," *Nature Nanotechnol.*, vol. 7, no. 8, pp. 494–498, Jun. 2012, doi: 10.1038/nnano.2012.96.

[4] K. F. Mak, M. Y. Sfeir, Y. Wu, C. H. Lui, J. A. Misewich, and T. F. Heinz, "Measurement of the optical conductivity of graphene," *Phys. Rev. Lett.*, vol. 101, no. 19, pp. 6797–6800, Nov. 2008, doi: 10.1103/PhysRevLett.101.196405.

[5] K. S. Novoselov, A. K. Geim, S. V. Morozov, D. Jiang, Y. Zhang, S. V. Dubonos, I. V. Grigorieva, and A. A. Firsov, "Electric field effect in atomically thin carbon films," *Science*, vol. 306, no. 5696, pp. 666–669, Oct. 2010, doi: 10.1126/science.1102896.

[6] F. Torrisi, T. Hasan, W. Wu, Z. Sun, A. Lombardo, T. S. Kulmala, G. W. Hsieh, S. Jung, F. Bonaccorso, and P. J. Paul, "Inkjet-printed graphene electronics," *ACS Nano*, vol. 6, no. 4, pp. 2992–3006, Mar. 2012, doi: 10.1021/nn2044609.

[7] Y. Wu, Y.-M. Lin, A. A. Bol, K. A. Jenkins, F. Xia, D. B. Farmer, Y. Zhu, and P. Avouris, "High-frequency, scaled graphene transistors on diamond-like carbon," *Nature*, vol. 472, no. 7341, pp. 74–78, Apr. 2011, doi: 10.1038/nature09979.

[8] Z. Yin, H. Li, H. Li, L. Jiang, Y. Shi, Y. Sun, G. Lu, Q. Zhang, X. Chen, and H. Zhang, "Single-layer MoS_2 phototransistors," *ACS Nano*, vol. 6, no. 1, pp. 74–80, Dec. 2011, doi: 10.1021/nn2024557.

[9] M. Buscema, M. Barkelid, V. Zwiller, H. S. van der Zant, G. A. Steele, and A. Castellanos-Gomez, "Large and tunable photothermoelectric effect in single-layer MoS_2," *Nano Lett.*, vol. 13, no. 2, pp. 358–363, Jan. 2013, doi: 10.1021/nl303321g.

[10] M. Fontana, T. Deppe, A. K. Boyd, M. Rinzan, A. Y. Liu, M. Paranjape, and P. Barbara, "Electron-hole transport and photovoltaic effect in gated MoS_2 Schottky junctions," *Sci. Rep.*, vol. 3, Apr. 2013, doi: 10.1038/srep01634.

[11] H. Fang, S. Chuang, T. C. Chang, K. Takei, T. Takahashi, and A. Javey, "High-performance single layered WSe_2 p-FETs with chemically doped contacts," *Nano Lett.*, vol. 12, no. 7, pp. 3788–3792, Jun. 2012, doi: 10.1021/nl301702r.

[12] M. S. Fuhrer and J. Hone, "Measurement of mobility in dual-gated MoS_2 transistors," *Nature Nanotechnol.*, vol. 8, no. 3, pp. 146–147, Mar. 2013, doi: 10.1038/nnano.2013.30.

[13] A. Castellanos-Gomez, L. Vicarelli, E. Prada, J. O. Island, K. L. Narasimha-Acharya, S. I. Blanter, D. J. Groenendijk, M. Buscema, G. A. Steele, and J. V. Alvarez, "Isolation and characterization of few-layer black phosphorus," *2D Mater.*, vol. 1, no. 2, pp. 025001-1–025001-18, Jun. 2014, doi: 10.1088/2053-1583/1/2/025001.

[14] K.-T. Lam, Z. Dong, and J. Guo, "Performance limits projection of black phosphorous field-effect transistors," *IEEE Electron Device Lett.*, vol. 35, no. 9, pp. 963–965, Jul. 2014, doi: 10.1109/LED.2014.2333368.

[15] A. Szabo, R. Rhyner, H. Carrillo-Nunez, and M. Luisier, "Phonon-limited performance of single-layer, single-gate black phosphorus n-and p-type field-effect transistors," presented at the IEDM Tech. Dig., Dec. 2015, pp. 12.1.1–12.1.4, doi: 10.1109/IEDM.2015.7409680.

[16] L. Li *et al.*, "Black phosphorus field-effect transistors," *Nature Nanotechnol.*, vol. 9, no. 5, pp. 372–377, Mar. 2014, doi: 10.1038/nnano.2014.35.

[17] M. Buscema, D. J. Groenendijk, S. I. Blanter, G. A. Steele, H. S. van der Zant, and A. Castellanos-Gomez, "Fast and broadband photoresponse of few-layer black phosphorus field-effect transistors," *Nano Lett.*, vol. 14, no. 6, pp. 3347–3352, May 2014, doi: 10.1021/nl5008085.

[18] M. Huang, M. Wang, C. Chen, Z. Ma, X. Li, J. Han, and Y. Wu, "Broadband black-phosphorus photodetectors with high responsivity," *Adv. Mater.*, vol. 28, no. 18, pp. 3481–3485, Mar. 2016, doi: 10.1002/adma.201506352.

[19] Q. Guo, A. Pospischil, M. Bhuiyan, H. Jiang, H. Tian, D. Farmer, B. Deng, C. Li, S.-J. Han, and H. Wang, "Black phosphorus mid-infrared photodetectors with high gain," *Nano Lett.*, vol. 16, no. 7, pp. 4648–4655, Jun. 2016, doi: 10.1021/acs.nanolett.6b01977.

[20] M. Si, L. Yang, Y. Du, and P. D. Ye, "Black phosphorus field-effect transistor with record drain current exceeding 1 A/mm," in *Proc. Device Res. Conf. (DRC)*, Jun. 2017, pp. 1–2, doi: 10.1109/DRC.2017.7999395.

[21] L. Yang, G. Qiu, M. Si, A. Charnas, C. Milligan, D. Zemlyanov, H. Zhou, Y. Du, Y. Lin, and W. Tsai, "Few-layer black phosporous PMOSFETs with BN/AI_2O_3 bilayer gate dielectric: Achieving Ion=850μA/μm, gm=340μS/μm, and Rc=0.58kO·μm," presented at the IEDM Tech. Dig., Dec. 2016, pp. 5.5.1–5.5.4, doi: 10.1109/IEDM.2016.7838354.

[22] T. Li, Z. Zhang, X. Li, M. Huang, S. Li, S. Li, and Y. Wu, "High field transport of high performance black phosphorus transistors," *Appl. Phy. Lett.*, vol. 110, no. 16, p. 163507, Apr. 2017, doi: 10.1063/1.4982033.

[23] N. Haratipour and S. J. Koester, "Ambipolar black phosphorus MOSFETs with record n-channel transconductance," *IEEE Electron Device Lett.*, vol. 37, no. 1, pp. 103–106, Jan. 2016, doi: 10.1109/LED.2015.2499209.

[24] Y. Deng, Z. Luo, N. J. Conrad, H. Liu, Y. Gong, S. Najmaei, P. M. Ajayan, J. Lou, X. Xu, and P. D. Ye, "Black phosphorus-monolayer MoS_2 van der waals heterojunction p-n diode," *ACS Nano*, vol. 8, no. 8, pp. 8292–8299, Jul. 2014, doi: 10.1021/nn5027388.

[25] F. Xia, H. Wang, and Y. Jia, "Rediscovering black phosphorus as an anisotropic layered material for optoelectronics and electronics," *Nature Commun.*, vol. 5, Jul. 2014, Art. no. 4458, doi: 10.1038/ncomms5458.

[26] Y. Yuan, B. Yu, J. Ahn, P. C. McIntyre, P. M. Asbeck, M. J. Rodwell, and Y. Taur, "A distributed bulk-oxide trap model for InGaAs MOS devices," *IEEE Trans. Electron Devices*, vol. 59, no. 8, pp. 2100–2106, May 2012, doi: 10.1109/TED.2012.2197000.

[27] M. Scarpino, S. Gupta, D. Lin, A. Alian, F. Crupi, N. Collaert, A. Thean, and E. Simoen, "Border traps in InGaAs nMOSFETs assessed by low-frequency noise," *IEEE Electron Device Lett.*, vol. 35, no. 7, pp. 720–722, May 2014, doi: 10.1109/LED.2014.2322388.

[28] J. Na, M.-K. Joo, M. Shin, J. Huh, J.-S. Kim, M. Piao, J.-E. Jin, H.-K. Jang, H. J. Choi, and J. H. Shim, "Low-frequency noise in multilayer MoS_2 field-effect transistors: The effect of high-*k* passivation," *Nanoscale*, vol. 6, no. 1, pp. 433–441, Oct. 2014, doi: 10.1039/C3NR04218A.

[29] Y. Du, L. Yang, H. Zhou, and P. D. Ye, "Performance enhancement of black phosphorus field-effect transistors by chemical doping," *IEEE Electron Device Lett.*, vol. 37, no. 4, pp. 429–432, Mar. 2016, doi: 10.1109/LED.2016.2535905.

[30] L. Li, M. Engel, D. B. Farmer, S.-J. Han, and H.-S. P. Wong, "High-performance p-type black phosphorus transistor with scandium contact," *ACS Nano*, vol. 10, no. 4, pp. 4672–4677, Mar. 2016, doi: 10.1021/acsnano.6b01008.

[31] M. Engel, M. Steiner, and P. Avouris, "Black phosphorus photodetector for multispectral, high-resolution imaging," *Nano Lett.*, vol. 14, no. 11, pp. 6414–6417, Oct. 2014, doi: 10.1021/nl502928y.

[32] Y. Deng, N. J. Conrad, Z. Luo, H. Liu, X. Xu, and D. Y. Peide, "Towards high-performance two-dimensional black phosphorus optoelectronic devices: The role of metal contacts," presented at the IEDM Tech. Dig., Dec. 2014, doi: 10.1109/IEDM.2014.7046987.

[33] N. Youngblood, C. Chen, S. J. Koester, and M. Li, "Waveguide-integrated black phosphorus photodetector with high responsivity and low dark current," *Nature Photon.*, vol. 9, p. 247, Mar. 2015, doi: 10.1038/nphoton.2015.23.

[34] J. Wu *et al.*, "Colossal ultraviolet photoresponsivity of few-layer black phosphorus," *ACS Nano*, vol. 9, no. 8, pp. 8070–8077, Jul. 2015, doi: 10.1021/acsnano.5b01922.

[35] G. Konstantatos *et al.*, "Ultrasensitive solution-cast quantum dot photodetectors," *Nature*, vol. 442, pp. 180–183, Jul. 2006, doi: 10.1038/nature04855.